

Modeling the Spectral Energy Distributions and Variability of Blazars

M. Boettcher

Astrophysical Institute, Department of Physics and Astronomy, Ohio University, Athens, OH 45701, USA

In this review, recent progress in theoretical models for the broadband (radio through γ -ray) emission from blazars are summarized. The salient features of both leptonic and hadronic models are reviewed. I present sample modeling results of spectral energy distributions (SEDs) of different types of *Fermi*-detected blazars along the traditional blazar sequence, using both types of models. In many cases, the SEDs of high-frequency peaked blazars (HBLs) have been found to be well represented by simple synchrotron + synchrotron self-Compton (SSC) models. However, a few HBLs recently discovered as very-high-energy (VHE) gamma-ray emitters by VERITAS are actually better represented by either external-Compton or hadronic models. Often, spectral modeling with time-independent single-zone models alone is not sufficient to constrain models, as both leptonic and lepto-hadronic models are able to provide acceptable fits to the overall SED. This degeneracy can be lifted by considering further constraints from spectral variability. Recent developments of time-dependent and inhomogeneous blazar models will be discussed, including detailed numerical simulations as well as a semi-analytical approach to the time-dependent radiation signatures of shock-in-jet models.

I. INTRODUCTION

Blazars (BL Lac objects and γ -ray loud flat spectrum radio quasars [FSRQs]) are the most extreme class of active galaxies known. Their broadband (from radio to γ -rays) continuum SEDs are dominated by non-thermal emission and consist of two distinct, broad components: a low-energy component from radio through UV or X-rays, and a high-energy component from X-rays to γ -rays (see, e.g., Figure 1).

Blazars are sub-divided into several types, defined by the location of the peak of the low-energy (synchrotron) SED component. Low-synchrotron-peaked (LSP) blazars, consisting of flat-spectrum radio quasars (FSRQs) and low-frequency peaked BL Lac objects (LBLs), have their synchrotron peak in the infrared regime, at $\nu_s \leq 10^{14}$ Hz. Intermediate-Synchrotron-Peaked (ISP) blazars, including LBLs and intermediate BL Lac objects (IBLs), have their synchrotron peak at optical – near-UV frequencies at 10^{14} Hz $< \nu_s \leq 10^{15}$ Hz, while High-Synchrotron-Peaked (HSP) blazars, which are almost all high-frequency-peaked BL Lac objects (HBL), have their synchrotron peak at X-ray energies with $\nu_s > 10^{15}$ Hz [2]. Such a sequence appears to be more physical than the historical distinction between quasars and BL Lac objects based on the equivalent width of optical emission lines [59], as the equivalent width is dependent on the strongly time-variable flux of the non-thermal continuum [51].

The blazar sequence had first been identified by [42], and associated also with a trend of overall decreasing bolometric luminosity as well as decreasing γ -ray dominance along the sequence FSRQ \rightarrow LBL \rightarrow HBL. According to this classification, the bolometric power output of FSRQs is strongly γ -ray dominated, especially during flaring states, while HBLs are expected to be always synchrotron dominated. However, while

the overall bolometric-luminosity trend still seems to hold, recently, even HBLs seem to undergo episodes of strong γ -ray dominance. A prominent example was the giant VHE γ -ray flare of the HBL PKS 2155-304 in 2006, during which the SED was strongly γ -ray dominated [12].

Figure 1 shows examples of blazar SEDs along the blazar sequence, from the FSRQ 3C279 (a), via the LBL BL Lacertae (b) and the IBL 3C 66A (c), to the HBL RGB J0710+591 (d). The sequence of increasing synchrotron peak frequency is clearly visible. However, the *Fermi* spectrum of the LBL BL Lacertae indicates a γ -ray flux clearly below the synchrotron level, while the SED of the IBL 3C 66A is clearly dominated by the *Fermi* γ -ray flux, in contradiction with the traditional blazar sequence.

Blazars are known to be variable at all wavelengths. Typically, the variability amplitudes are the largest and variability time scales are the shortest at the high-frequency ends of the two SED components. In HBLs, this refers to the X-ray and VHE γ -ray regimes. High-energy variability in some HBLs (PKS 2155-305, Mrk 501, Mrk 421) has been observed on time scales down to just a few minutes [10, 13, 41]. The flux variability of blazars is often accompanied by spectral changes which are sometimes associated with inter-band or intra-band time lags. In a few HBLs (especially, Mrk 421), variability patterns have been found which can be characterized as spectral hysteresis in hardness-intensity diagrams [e.g., 43, 57, 85, 91]. However, even within the same object this feature tends not to be persistent over multiple observations. Also in other types of blazars, hints of time lags between different observing bands are occasionally found in individual observing campaigns (e.g., [28, 54]), but the search for time-lag patterns persisting throughout multiple years has so far remained unsuccessful [see, e.g., 53, for a systematic search for time lags between optical, X-ray and γ -ray emission in the quasar

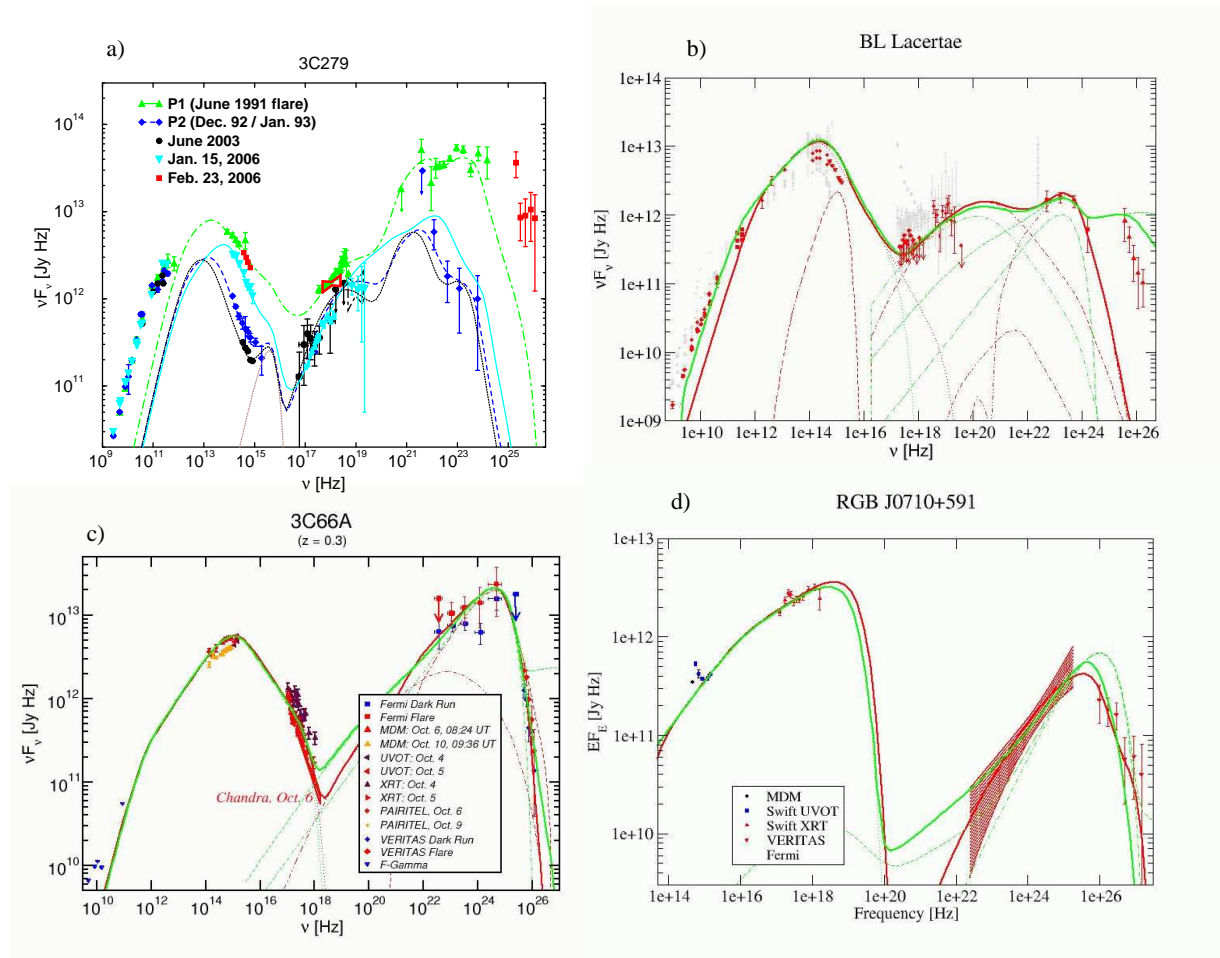


FIG. 1: Spectral energy distributions of four sub-classes of blazars: a) the FSRQ 3C279 (from [36]), b) the LBL BL Lacertae, (data from [2]), c) the intermediate BL Lac 3C66A (data from [3]), and d) the HBL RGB J0710+591 (data from [8]). In Panel a) (3C279), lines are one-zone leptonic model fits to SEDs at various epochs shown in the figure. In all other panels, red lines are fits with a leptonic one-zone model; green lines are fits with a one-zone lepto-hadronic model.

3C279].

II. LEPTONIC AND HADRONIC BLAZAR MODELS

The high apparent bolometric luminosities (assuming isotropic emission), rapid variability, and apparent superluminal motions of radio components in blazar jets provide compelling evidence that the nonthermal continuum emission of blazars is produced in $\lesssim 1$ light day sized emission regions, propagating relativistically with velocity $\beta_{\Gamma}c$ along a jet directed at a small angle θ_{obs} with respect to our line of sight [e.g., 79]. Let $\Gamma = (1 - \beta_{\Gamma}^2)^{-1/2}$ be the bulk Lorentz factor of the emission region, then Doppler boosting is determined by the Doppler factor $D = (\Gamma[1 - \beta_{\Gamma} \cos \theta_{\text{obs}}])^{-1}$. In the following, primes denote quantities in the co-moving frame of the emission region. The observed

frequency ν_{obs} is related to the emitted frequency through $\nu_{\text{obs}} = D \nu' / (1 + z)$, where z is the redshift of the source. The energy fluxes are connected through $F_{\nu_{\text{obs}}}^{\text{obs}} = D^3 F_{\nu'}'$. Intrinsic variability on a co-moving time scale t'_{var} will be observed on a time scale $t_{\text{var}}^{\text{obs}} = t'_{\text{var}} (1 + z) / D$. Using the latter transformation along with causality arguments, any observed variability leads to an upper limit on the size scale of the emission region through $R \lesssim c t_{\text{var}}^{\text{obs}} D / (1 + z)$.

It is generally agreed that the low-frequency component in the blazar SED arises from synchrotron emission of relativistic electrons. However, there are two fundamentally different approaches concerning the high-energy emission. If protons are not accelerated to ultrarelativistic energies (exceeding the threshold for $p\gamma$ pion production on synchrotron and/or external photons), the high-energy radiation will be dominated by Compton emission from ultrarelativistic electrons and/or pairs (leptonic models). In the oppo-

site case, the high-energy emission will be dominated by cascades initiated by $p\gamma$ pair and pion production as well as proton, π^\pm , and μ^\pm synchrotron radiation, while primary leptons are still responsible for the low-frequency synchrotron emission (hadronic models). The following sub-sections provide a brief overview of the main radiation physics aspects of both leptonic and hadronic models. A more in-depth review of the radiation physics in relativistic jets can be found in [33].

When fitting SEDs of blazars, consideration should be given to the energy balance between the magnetic field and the particle content in the jet, as this contains information on the jet launching and acceleration mechanisms. If the relativistic jets of AGN are powered by the rotational energy of the central black hole [23], the jets are expected to be initially Poynting-flux dominated. The energy thus carried primarily in the form of magnetic fields then needs to be transferred to relativistic particles which can then produce the observed high-energy emission. This energy conversion is expected to cease when the energy densities in the magnetic field and in relativistic particles approach equipartition. In this scenario, the jets are therefore not expected to become matter dominated within the central few parsecs of AGN, where the high-energy emission in blazars is believed to be produced [63]. Also, if magnetic pressure plays an essential role in collimating and confining the jets out to pc or kpc scales, the energy density (and hence pressure) of particles in the jet can not dominate over the magnetic-field pressure since otherwise the jets would simply expand conically.

If SED fits require far sub-equipartition magnetic fields, this may indicate that the jets are magneto-hydrodynamically powered by the accretion flow. In this case, magnetic fields may be self-generated in shear flows in the case of a fast inner spine surrounded by a slower, mildly relativistic outer flow (sheath). Kelvin-Helmholtz type instabilities can then lead to anisotropic particle acceleration, and the self-generated magnetic fields are expected to remain below equipartition with the thermal energy carried in the flow [19, 61].

A. Leptonic models

In leptonic models, the high-energy emission is produced via Compton upscattering of soft photons off the same ultrarelativistic electrons which are producing the synchrotron emission. Both the synchrotron photons produced within the jet [SSC = Synchrotron Self-Compton: 25, 66, 67], and external photons (EC = External Compton) can serve as target photons for Compton scattering. Possible sources of external seed photons include the accretion disk radiation [e.g., 37, 38], reprocessed optical – UV emission from

circumnuclear material [e.g., the BLR; 22, 39, 46, 80], infrared emission from warm dust [24], or synchrotron emission from other (faster/slower) regions of the jet itself [44, 49].

If the observed blazar emission were arising in a stationary emission region (whose size is constrained by causality arguments), its compactness would, in many cases, be too large for high-energy γ -rays to escape from it. This problem is overcome by relativistic Doppler boosting so that model fits can be achieved with parameters such that the $\gamma\gamma$ opacity of the emission region is low throughout most of the high-energy spectrum. However, at the highest photon energies, this effect may make a non-negligible contribution to the formation of the emerging spectrum [11] and lead to the re-processing of some of the radiated power towards lower frequencies. $\gamma\gamma$ absorption within the AGN may also occur on photons external to the emission region, as required to be present if γ -rays are produced through the EC mechanism [e.g. 62, 74, 76]. This absorption process might lead to Compton supported pair cascades which are expected to release their peak power at MeV – GeV energies [e.g., 77, 78].

Also the deceleration of the jets may have a significant impact on the observable properties of blazar emission through the radiative interaction of emission regions with different speed [44, 48]. The deceleration of the high-energy emission region is expected to cause characteristic variability features which may be reminiscent of those seen in gamma-ray burst light curves [32]. Varying Doppler factors may also be a result of a slight change in the jet orientation without a substantial change in speed, e.g., in a helical-jet configuration [e.g., 88]. In the case of ordered magnetic-field structures in the emission region, such a helical configuration should have observable synchrotron polarization signatures, such as the prominent polarization-angle swing recently observed in conjunction with an optical + *Fermi* γ -ray flare of 3C 279 [1].

In the simplest models, the underlying lepton (electrons and/or positrons) distribution is ad-hoc pre-specified, either as a single or broken power-law with a low- and high-energy cut-off. While leptonic models under this assumption have been successful in modeling blazar SEDs [e.g., 47], they lack a self-consistent basis for the shape of the electron distribution. A more realistic approach consists of the self-consistent steady-state solution of the Fokker-Planck equation governing the evolution of the electron distribution function, including a physically motivated (e.g., from shock-acceleration theory) acceleration of particles and all relevant radiative and adiabatic cooling mechanisms [e.g., 6, 50, 90]. The model described in [6], based on the time-dependent model of [26] [see also 34], has been used to produce the leptonic model fits shown in Fig. 1.

In order to reproduce not only broadband SEDs, but also variability patterns, the time-dependent elec-

tron dynamics and radiation transfer problem has to be solved self-consistently. Such time-dependent SSC models have been developed by, e.g., [57, 60, 68, 82]. External radiation fields have been included in such treatments in, e.g., [26, 81, 83].

Leptonic models have generally been very successfully applied to model the SEDs and (in few cases) spectral variability of blazars. The radiative cooling time scales (in the observers’s frame) of synchrotron-emitting electrons in a typical $B \sim 1$ G magnetic field are of the order of several hours – ~ 1 d at optical frequencies and $\lesssim 1$ hr in X-rays and hence compatible with the observed intra-day variability. However, the recent observation of extremely rapid VHE γ -ray variability on time scales of a few minutes poses severe problems to simple one-zone leptonic emission models. Even with large bulk Lorentz factors of ~ 50 , causality requires a size of the emitting region that might be smaller than the Schwarzschild radius of the central black hole of the AGN [21]. As a possible solution, it has been suggested [87] that the γ -ray emission region may, in fact, be only a small spine of ultrarelativistic plasma within a larger, slower-moving jet. Such fast-moving small-scale jets could plausibly be powered by magnetic reconnection in a Poynting-flux dominated jet, as proposed by [45].

B. Hadronic models

If a significant fraction of the jet power is converted into the acceleration of relativistic protons in a strongly magnetized environment, reaching the threshold for $p\gamma$ pion production, synchrotron-supported pair cascades will develop, initiated by primary π^0 decay photons and synchrotron emission from secondary pions, muons and electrons/positrons at ultra-high γ -ray energies, where the emission region is highly opaque to $\gamma\gamma$ absorption [64, 65]. The acceleration of protons to the necessary ultrarelativistic energies ($E_p^{\max} \gtrsim 10^{19}$ eV) requires high magnetic fields of several tens of Gauss to constrain the Larmor radius $R_L = 3.3 \times 10^{15} B_1^{-1} E_{19}$ cm, where $B = 10 B_1$ G, and $E_p = 10^{19} E_{19}$ eV, to be smaller than the size of the emission region (typically inferred to be $R \lesssim 10^{16}$ cm from the observed variability time scale). In the presence of such high magnetic fields, the synchrotron radiation of the primary protons [9, 71] and of secondary muons and mesons [71–73, 75] must be taken into account in order to construct a self-consistent synchrotron-proton blazar (SPB) model. Electromagnetic cascades can be initiated by photons from π^0 -decay (“ π^0 cascade”), electrons from the $\pi^\pm \rightarrow \mu^\pm \rightarrow e^\pm$ decay (“ π^\pm cascade”), p -synchrotron photons (“ p -synchrotron cascade”), and μ -, π - and K -synchrotron photons (“ μ^\pm -synchrotron cascade”).

[72] and [73] have shown that the “ π^0 cascades” and “ π^\pm cascades” from ultra-high energy protons

generate featureless γ -ray spectra, in contrast to “ p -synchrotron cascades” and “ μ^\pm -synchrotron cascades” that produce a two-component γ -ray spectrum. In general, direct proton and μ^\pm synchrotron radiation is mainly responsible for the high energy bump in blazars, whereas the low energy bump is dominated by synchrotron radiation from the primary e^- , with a contribution from secondary electrons.

Hadronic blazar models have so far been very difficult to investigate in a time-dependent way because of the very time-consuming nature of the required Monte-Carlo cascade simulations. In general, it appears that it is difficult to reconcile very rapid high-energy variability with the radiative cooling time scales of protons, e.g., due to synchrotron emission, which is $t_{\text{sy}}^{\text{obs}} = 4.5 \times 10^5 (1+z) D_1^{-1} B_1^{-2} E_{19}^{-1}$ s [9], i.e., of the order of several days for ~ 10 G magnetic fields and typical Doppler factors $D = 10 D_1$. However, rapid variability on time scales shorter than the proton cooling time scale may be caused by geometrical effects, for example in a helical jet.

In order to avoid time-consuming Monte-Carlo simulations of the hadronic processes and cascades involved in lepto-hadronic models, one may consider a simplified prescription of the hadronic processes. [58] have produced analytic fit functions to Monte-Carlo generated results of hadronic interactions using the SOFIA code [70]. Those fits describe the spectra of the final decay products, such as electrons, positrons, neutrinos, and photons from π^0 decay. This neglects the possibility of substantial synchrotron losses to muons and pions before they decay. Since the muon life time is longer than the pion life time, the more stringent condition is given by the requirement that $t_{\text{sy},\mu} \gg t_{\text{d},\mu}$, where t_{sy} and t_{d} denote the synchrotron and decay time scales, respectively. This can be translated into the requirement that $B \ll 5.6 \gamma_{\text{p,max},10}^{-1}$ G, where $\gamma_{\text{p,max},10}$ is the Lorentz factor of the highest-energy protons in units of 10^{10} . [55] have developed analytical fits to the secondary-production spectra in hadronic processes for all individual steps, thus allowing one to take muon and pion synchrotron (and Compton) emission into account properly.

A hadronic blazar model based on the templates of [58] has been developed by [34] [see also 30]. This model employs a semi-analytical solution for UHE γ -ray induced, synchrotron-supported pair cascades. The hadronic fits shown in Fig 1, b) – d) have been performed with this model. As the low-frequency component is electron-synchrotron emission from primary electrons, it is not surprising that virtually identical fits to the synchrotron component can be provided in both types of models. In the high-frequency component, strongly peaked spectral shapes, as, e.g., in 3C 66A and RGB J0710+591 require a strong proton-synchrotron dominance with the cascading of higher-energy (\gg TeV) emission only making a minor contribution to the high-energy emission. This,

in fact, makes it difficult to achieve a substantial extension of the escaping high-energy emission into the > 100 GeV VHE γ -ray regime. In objects with a smoother high-energy SED, e.g., BL Lacertae in Fig. 1b, a substantially larger contribution from cascade emission (and leptonic SSC emission) is allowed to account for a relatively high level of hard X-ray / soft γ -ray emission. This also allows for a substantial extension of the γ -ray spectrum into the VHE regime.

III. SED FITS ALONG THE BLAZAR SEQUENCE

In the framework of leptonic models, the blazar sequence LSP \rightarrow ISP \rightarrow HSP is often modeled through a decreasing contribution of external radiation fields to radiative cooling of electrons and associated EC γ -ray emission [47]. In this sense, HBLs have traditionally been well represented by pure synchrotron-self-Compton models, while FSRQs usually require a substantial EC component. This interpretation is consistent with the observed strong emission lines in FSRQs, which are absent in BL Lac objects. At the same time, the denser circumnuclear environment in quasars might also lead to a higher accretion rate and hence a more powerful jet, consistent with the overall trend of bolometric luminosities along the blazar sequence. This may even be related to an evolutionary sequence from FSRQs to HBLs governed by the gradual depletion of the circumnuclear environment [27].

However, in this interpretation, it would be expected that mostly HBLs (and maybe IBLs) should be detectable as emitters of VHE γ -rays since in LBLs and FSRQs, electrons are not expected to reach \sim TeV energies. This paradigm has been undermined by the recent VHE γ -ray detections of lower-frequency peaked objects such as W Comae [4], 3C66A [5], PKS 1424+240 [7], BL Lacertae [14], S5 0716+714 [20], and even the FSRQs 3C 279 [15], PKS 1222+21 [16] and PKS 1510-089 [89].

The overall SEDs of IBLs detected by VERITAS could still be fit satisfactorily with a purely leptonic model. Fitting the SEDs of the IBLs 3C66A and W Comae with a pure SSC model, while formally possible, would require rather extreme parameters. In particular, magnetic fields several orders of magnitude below equipartition would be needed, which might pose a severe problem for jet collimation (see the discussion in Section II). Much more natural fit parameters can be adopted when including an EC component with an infrared radiation field as target photons [3, 6].

In [29] it has been demonstrated that the VHE γ -ray detection of the FSRQ 3C 279 poses severe problems for any variation of a single-zone leptonic jet model. The fundamental problem for the leptonic model in-

terpretation is the extremely wide separation between the synchrotron and γ -ray peak frequencies. In a single-zone SSC interpretation this would require a very high Lorentz factor of electrons at the peak of the electron distribution and, in turn, an extremely low magnetic field. In an EC interpretation the SSC component, usually dominating the X-ray emission in leptonic fits to FSRQs like 3C 279, is too far suppressed to model the simultaneous RXTE spectrum. As an alternative, the optical emission could be produced in a separate emission component. A pure SSC fit to the X-ray and γ -ray component is technically possible, but also requires a far sub-equipartition magnetic field. Much more natural parameters could be achieved in a fit with the synchrotron-proton-blazar model of [73].

A. HBLs disfavouring SSC

Until very recently, the SEDs of essentially all HBLs detected in VHE γ -rays could be well modelled using simple leptonic SSC models. The most attractive feature of this model is its relative simplicity, requiring only a small number of fit parameters. If the peak frequencies and corresponding fluxes in a blazar SED are well measured and an additional constraint on the emission region size can be obtained from rapid variability, then all relevant parameters can be uniquely determined [e.g., 86]. However, recent new discoveries by VERITAS with good simultaneous or quasi-simultaneous multiwavelength coverage provided strongly constraining SEDs that were difficult to reproduce with such a model.

The HBL RX J0648.7+1516 ($z = 0.179$) was detected as a VHE γ -ray source by VERITAS in 2010 March – April [17]. Simultaneous multiwavelength coverage was provided by *Fermi*-LAT, *Swift* XRT and UVOT and the MDM Observatory (optical B, V, R bands). The resulting SED is shown in the left panel of Figure 2. An attempt to fit this SED with a pure SSC model clearly overshoots both the simultaneous *Fermi* upper limits and the 2-year average spectrum. This is a consequence of the apparent sharp spectral break between the *Fermi* and VERITAS energy ranges, which is not consistent with the smooth curvature of an SSC spectrum (resulting from the broad ranges of scattering electron energies and synchrotron seed photon frequencies, in combination with the gradual onset of Klein-Nishina effects). A much more satisfactory leptonic fit can be achieved when allowing for an EC contribution to the γ -ray emission. In the fit shown by the dot-dashed curve in the left panel of Fig. 2, an external blackbody radiation field at a temperature of $T = 1000$ K has been assumed, which could result from an infrared-emitting dust region around the AGN. Its luminosity corresponds to a flux of $\nu F_{\nu}^{\text{IR}} \lesssim 10^9$ Jy Hz, in agreement with its non-

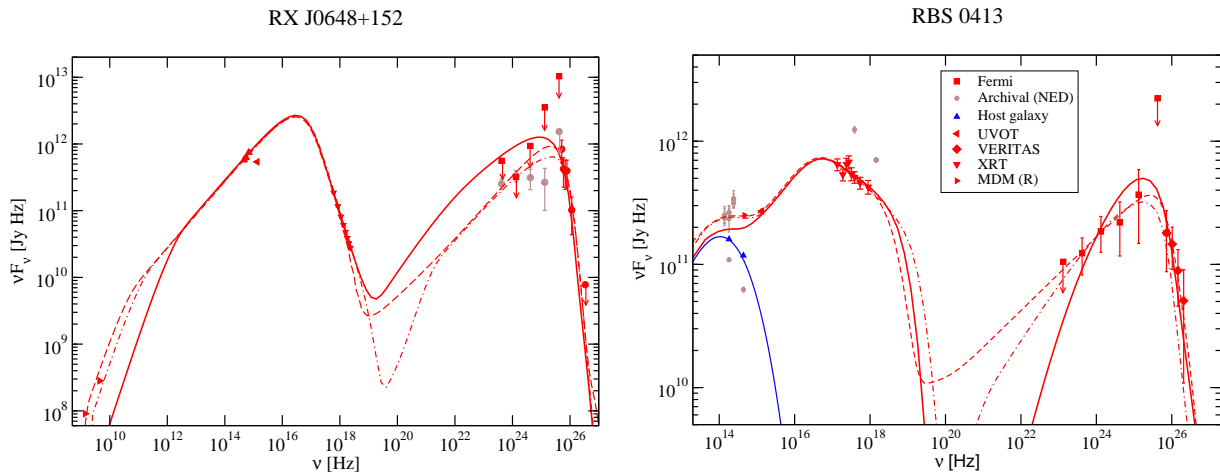


FIG. 2: Spectral energy distributions of the HBLs RX J0648.7+1516 [left; 17] and RBS 0413 [right; 18]. The *Fermi* upper limits for RX J0648.7+1516 correspond to the ~ 2 months time window simultaneous with the VERITAS observations, while the brown *Fermi* points show the 2-year average spectrum. The solid curve indicates a pure leptonic SSC fit. The dashed dot-dashed curve is a leptonic SSC + EC fit, while the dashed curve shows a fit with the semi-analytical hadronic model described in Section II B. See text for details of the individual fits. The blue curve in the right panel represents a phenomenological representation of the (thermal dominated) host-galaxy emission.

detection in the SED.

Alternatively, the hadronic model described above also provides a satisfactory fit to the SED (the dashed curve in the left panel of Fig. 2). The model requires protons to be accelerated up to $E_{p,\max} = 1.5 \times 10^{19}$ eV, with a total kinetic luminosity in relativistic protons of $L_p = 2 \times 10^{45}$ erg/s. While hadronic models often suffer from extreme power requirements, this appears to be a very reasonable jet power. The magnetic field of $B = 10$ G is slightly above equipartition with the energy content in relativistic protons.

The HBL RBS 0413 ($z = 0.19$) was detected by VERITAS in data accumulated between 2008 September and 2010 January. Contemporaneous multiwavelength coverage was provided by *Fermi*-LAT, *Swift* XRT and UVOT, and MDM (R-band). A leptonic SSC model fit (solid curve in the right panel of Fig. 2) produces a GeV γ -ray spectrum significantly harder than indicated by *Fermi*-LAT, and requires a magnetic field energy density a factor $\sim 6 \times 10^{-2}$ below equipartition. A much more satisfactory representation of the entire SED (including the *Fermi*-LAT spectrum), can be achieved by including an EC component with a thermal blackbody radiation field at $T = 1.5 \times 10^3$ K. This is shown by the dot-dashed curve in the right panel of Figure 2). Parameters in almost exact equipartition between the magnetic field and the relativistic electron population can be chosen, and the postulated infrared radiation field corresponds to a flux of $\nu F_\nu^{\text{IR}} \sim 5 \times 10^8$ JyHz, consistent with the absence of direct evidence for it in the infrared spectrum of the source.

The dashed curve in the right panel of Fig. 2 shows a hadronic fit to the SED of RBS 0413, which also

provides a better representation than the pure SSC model. For this fit, protons need to be accelerated to $E_{p,\max} = 1.6 \times 10^{19}$ eV with a kinetic power of $L_p = 2 \times 10^{46}$ erg/s. The magnetic field of $B = 30$ G is in almost exact equipartition with the energy content in relativistic protons.

Thus, both RX J0648.7+1516 and RBS 0413 exhibit SEDs that disfavor a pure leptonic single-zone SSC interpretation, while both an EC model using a thermal infrared radiation field, and a hadronic model provide convincing fits. Both EC and hadronic model fits can be achieved with reasonable energy requirements and parameters close to equipartition between the magnetic field and the dominant relativistic particle population.

IV. INHOMOGENEOUS JET MODELS

The complicated and often inconsistent variability features found in blazars provide a strong motivation to investigate jet models beyond a simple, spherical, one-zone geometry. The idea behind phenomenological multi-zone models like the spine-sheath model of [87] or the decelerating-jet model of [44] was that differential relativistic motion between various emission zones will lead to Doppler boosting of one zone's emission into the rest frame of another zone. This can reduce the requirements of extreme bulk Lorentz (and Doppler) factors inferred from simple one-zone leptonic modeling of rapidly variable VHE γ -ray blazars, such as Mrk 501 or PKS 2155-304, and has led to successful model fits to the SEDs of those sources with much more reasonable model parameters.

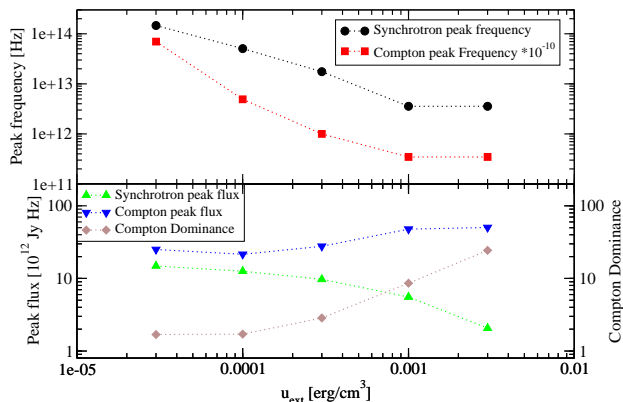


FIG. 3: Dependence of the SED characteristics of time-averaged spectra from the internal-shock model, on the external radiation energy density u_{ext} .

However, the models mentioned above do not treat the radiation transport and electron dynamics in a time-dependent way and do therefore not make any robust predictions concerning variability and inter-band cross-correlations and time lags. In order to address those issues, much work has recently been devoted to the investigation of the radiative and timing signatures of shock-in-jet models, which will be summarized in the following sub-section.

A. Shock-in-jet models

Early versions of shock-in-jet models were developed with focus on explaining radio spectra of extragalactic jets, e.g., by [67]. Their application to high-energy spectra of blazars was proposed by [84]. Detailed treatments of the electron energization and dynamics and the radiation transfer in a standing shock (Mach disk) in a blazar jet were developed by [52, 82, 83]. The internal-shock model discussed in [69] and [56] assumes that the central engine is intermittently ejecting shells of relativistic plasma at varying speeds, which subsequently collide. Such models have had remarkable success in explaining SEDs and time lag features of generic blazars.

The realistic treatment of radiation transfer in an internal-shock model for a blazar requires the time-dependent evaluation of retarded radiation fields originating from all parts of the shocked regions of the jet. The model system is therefore highly non-linear and can generally only be solved using numerical simulations (e.g., [52, 69, 82]). As the current detailed internal-shock models employ either full expressions or accurate approximations to the full emissivities of synchrotron and Compton emission, a complete simulation of the time-dependent spectra and light curves

is time-consuming and does therefore generally not allow to efficiently explore a large parameter space. General patterns of the SED, light curves and expected time lags between different wavelength bands have been demonstrated for very specific, but observationally very poorly constrained, sets of parameters. The most detailed treatment of the radiation-transfer aspect in the context of this models, including all light-travel time effects, has been presented in [35], who employ a time-dependent multi-zone Monte-Carlo (for the radiation transfer) and Fokker-Planck (for electron dynamics) code.

In order to be able to explore timing signatures of the internal-shock model for blazars on the basis of a broad parameter study, [31] have developed a semi-analytical scheme for this model. The time- and space-dependent electron spectra, affected by shock acceleration behind the forward and reverse shocks, and subsequent radiative cooling, are calculated fully analytically. Taking into account all light travel time effects, the observed synchrotron and external-Compton spectra are also evaluated fully analytically, using a δ -function approximation to the emissivities. The evaluation of the SSC emission still requires a two-dimensional numerical integration.

This semi-analytical model allowed the authors to efficiently scan a substantial region of parameter space and discuss the dependence on the characteristics of time-averaged SEDs, as well as cross-band correlations and time lags. As an example, Fig. 3 shows the dependence of the SED characteristics on the external radiation field energy density, u_{ext} . In the classical interpretation of the blazar sequence, an increasing u_{ext} corresponds to a transition from BL Lac spectral characteristics to FSRQ-like characteristics. The decreasing synchrotron peak frequency and increasing Compton dominance found in the parameter study are reproducing this effect.

From the internal-shock simulations, energy-dependent light curves could be extracted. Using the standard Discrete Correlation Function (DCF: [40]) analysis, inter-band time lags could be extracted for any set of parameters. Fig. 4 shows the dependence of the inter-band time lags between optical, X-ray and *Fermi* γ -ray light curves (top panel) and the quality of the cross correlation, characterized by the peak value of the DCF (bottom panel) as a function of the external radiation energy density.

One of the most remarkable results of this study was that only slight changes in physical parameters can lead to substantial changes of the inter-band time lags and even a reversal of the sign of the lags. This may explain the lack of consistency of lags even within the same source.

Acknowledgments

This work has been supported by NASA through Astrophysics Theory Program grant NNX10AC79G and *Fermi* Guest Investigator grants NNX09AT82G and NNX10AO49G.

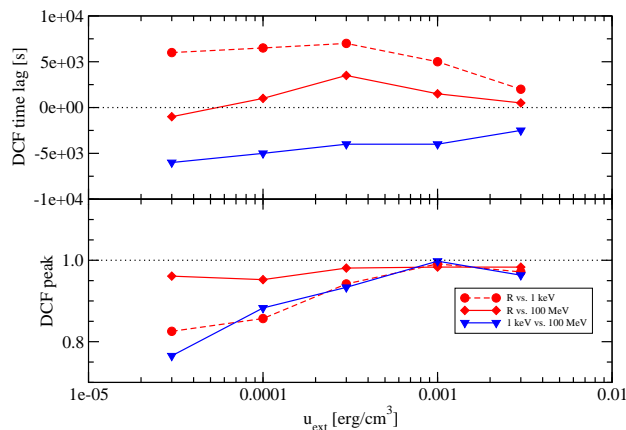
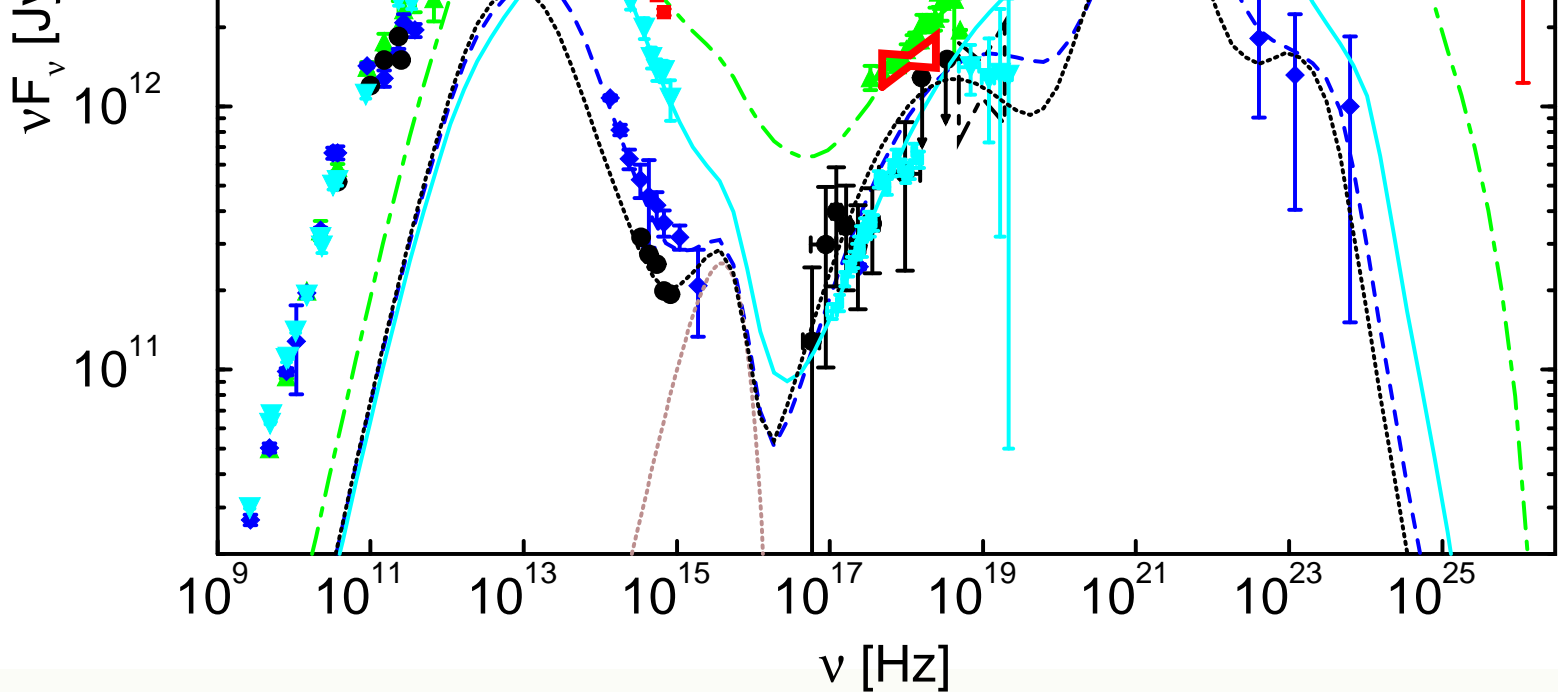


FIG. 4: Dependence on inter-band cross correlations and time lags on the external radiation energy density.

-
- [1] Abdo, A. A., et al., 2010, *Nature*, **463**, 919
[2] Abdo, A. A., et al., 2010b, *ApJ*, **716**, 30
[3] Abdo, A. A., et al., 2011, *ApJ*, **726**, 43
[4] Acciari, V. A., 2008, *ApJ*, **684**, L73
[5] Acciari, V. A., 2009a, *ApJ*, **693**, L104
[6] Acciari, V. A., 2009b, *ApJ*, **707**, 612
[7] Acciari, V. A., et al., 2010a, *ApJ*, **708**, L100
[8] Acciari, V. A., et al., 2010b, *ApJ*, **715**, L49
[9] Aharonian, F. A., 2000, *New Astron.*, **5**, 377
[10] Aharonian, F. A., et al., 2007, *ApJ*, **664**, L71
[11] Aharonian, F. A., Khangulyan, D., & Costamante, L., 2008, *MNRAS*, **387**, 1206
[12] Aharonian, F. A., et al., 2009, *A&A*, **502**, 749
[13] Albert, J., et al., 2007a, *ApJ*, **669**, 862
[14] Albert, J., et al., 2007b, *ApJ*, **66**, L17
[15] Albert, J., et al., 2008, *Science*, **320**, 1752
[16] Aleksic, J., 2011, *ApJ*, **730**, L8
[17] Aliu, E., et al., 2011, *ApJ*, **742**, 127
[18] Aliu, E., et al., 2012, *ApJ*, **750**, 94
[19] Alves, E. P., et al., 2011, arXiv:1107.6037
[20] Anderhub, H., et al., 2009, *ApJ*, **704**, L129
[21] Begelman, M. C., Fabian, A. C., & Rees, M. J., 2008, *MNRAS*, **384**, L19
[22] Blandford, R. D., & Levinson, A., 1995, *ApJ*, **441**, 79
[23] Blandford, R. D., & Znajek, R. L., 1977, *MNRAS*, **179**, 433
[24] Blażejowski, M., et al., 2000, *ApJ*, **545**, 107
[25] Bloom, S. D., & Marscher, A. P., 1996, *ApJ*, **461**, 657
[26] Böttcher, M., & Chiang, J., 2002, *ApJ*, **581**, 127
[27] Böttcher, M., & Dermer, C. D., 2002, *ApJ*, **564**, 86
[28] Böttcher, M., et al., 2007, *ApJ*, **670**, 968
[29] Böttcher, M., Reimer, A., & Marscher, A. P., 2009, *ApJ*, **703**, 1168
[30] Böttcher, M., 2010, in proc. of “*Fermi* Meets *Jansky*”, Bonn, Germany, 2010; Eds. T. Savolainen, E. Ros, R. W. Porcas, J. A. Zensus; p. 41
[31] Böttcher, M., & Dermer, C. D., 2010, *ApJ*, **711**, 445
[32] Böttcher, M., & Principe, D., 2009, *ApJ*, **692**, 1374
[33] Böttcher, M., & Reimer, A., 2012, “Radiation Processes”, in “*Relativistic Jets from Active Galactic Nuclei*”, Eds. M. Böttcher, D. Harris, H. Krawczynski; Wiley-VCH
[34] Böttcher, M., Reimer, A., Sweeney, K., & Prakash, A., 2012, in preparation
[35] Chen, X., et al., 2011, *MNRAS*, **416**, 2368
[36] Collmar, W., et al., 2010, *A&A*, **522**, A66
[37] Dermer, C. D., Schlickeiser, R., & Mastichiadis, A., 1992, *A&A*, **256**, L27
[38] Dermer, C. D., & Schlickeiser, R., 1993, *ApJ*, **416**, 458
[39] Dermer, C. D., Sturmer, S. J., & Schlickeiser, R., 1997, *ApJS*, **109**, 103
[40] Edelson, R. A., & Krolik, J. H., 1988, *ApJ*, **333**, 646
[41] Fortson, L., for the VERITAS Collaboration, 2011, *BAAS*, # **217**, vol. **43**, # 408.05
[42] Fossati, G., et al., 1998, *MNRAS*, **299**, 433
[43] Fossati, G., et al., 2000, *ApJ*, **541**, 166
[44] Georganopoulos, M., & Kazanas, D., 2003, *ApJ*, **594**, L27
[45] Giannios, D., Uzdensky, D. A., & Begelman, M. C., 2009, *MNRAS*, **395**, L29
[46] Ghisellini, G., & Madau, P. 1996, *MNRAS*, **280**, 67
[47] Ghisellini, G., et al., 1998, *MNRAS*, **301**, 451
[48] Ghisellini, G., Tavecchio, F., & Chiaberge, M., 2005, *A&A*, **432**, 401
[49] Ghisellini, G., & Tavecchio, F., 2008, *MNRAS*, **386**, L28
[50] Ghisellini, G., & Tavecchio, F., 2009, *MNRAS*, **397**, 985
[51] Giommi, P., et al., 2012, *MNRAS*, in press (arXiv:1110.4706)
[52] Graff, P. B., Georganopoulos, M., Perlman, E. S., & Kazanas, D., 2008, *ApJ*, **689**, 68
[53] Hartman, R. C., et al., 2001, *ApJ*, **558**, 583
[54] Horan, D., et al., 2009, *ApJ*, **695**, 596
[55] Hümmer, S., Rügner, M., Spanier, F., & Winter, W.,

- 2010, *ApJ*, **721**, 630
- [56] Joshi, M., & Böttcher, M., 2011, *ApJ*, **727**, 21
- [57] Kataoka, J., et al., 2000, *ApJ*, **528**, 243
- [58] Kelner, S. R., & Aharonian, F. A., 2008, *Phys. Rev. D.*, **78**, 034013
- [59] Landt, H., et al., 2004, *MNRAS*, **351**, 83
- [60] Li, H., & Kusunose, M., 2000, *ApJ*, **536**, 729
- [61] Liang, E., Böttcher, M., & Smith, I. A., 2011, arXiv:1111.3326
- [62] Liu, H., Bai, J. M., & Ma, L., 2008, *ApJ*, **688**, 148
- [63] Lyubarsky, Y. E., 2011, *MNRAS*, **402**, 353
- [64] Mannheim, K., & Biermann, P. L., 1992, *A&A*, **253**, L21
- [65] Mannheim, K., 1993, *A&A*, **221**, 211
- [66] Maraschi, L., Celotti, A., & Ghisellini, G., 1992, *ApJ*, **397**, L5
- [67] Marscher, A. P., & Gear, W. K., 1985, *ApJ*, **298**, 114
- [68] Mastichiadis, A., & Kirk, J. G., 1997, *A&A*, **320**, 19
- [69] Mimica, P., Aloy, M. A., Müller, E., & Brinkmann, W., 2004, *A&A*, **418**, 947
- [70] Mücke, A., et al., 2000, *Comp. Phys. Comm.*, **124**, 290
- [71] Mücke, A., & Protheroe, R. J., 2000, *AIP Conf. Proc.*, **515**, 149
- [72] Mücke, A., & Protheroe, R. J., 2001, *Astropart. Phys.*, **15**, 121
- [73] Mücke, A., et al., 2003, *Astropart. Phys.*, **18**, 593
- [74] Poutanen, J., & Stern, B., 2010, *ApJ*, **717**, L118
- [75] Rachen, J., & Mészáros, P., 1998, *Phys. Rev. D*, **58**, 123005
- [76] Reimer, A., 2007, *ApJ*, **665**, 1023
- [77] Roustazadeh, P., & Böttcher, M., 2010, *ApJ*, **717**, 468
- [78] Roustazadeh, P., & Böttcher, M., 2011, *ApJ*, **728**, 134
- [79] Savolainen, T., et al., 2010, *A&A*, **512**, A24
- [80] Sikora, M., Begelman, M., & Rees, M. 1994, *ApJ*, **421**, 153
- [81] Sikora, M., et al., 2001, *ApJ*, **554**, 1
- [82] Sokolov, A., Marscher, A. P., & McHardy, I. A., 2004, *ApJ*, **613**, 725
- [83] Sokolov, A., & Marscher, A. P., 2005, *ApJ*, **629**, 52
- [84] Spada, M., Ghisellini, G., Lazzati, D., & Celotti, A., 2001, *MNRAS*, **325**, 1559
- [85] Takahashi, T., et al., 1996, *ApJ*, **470**, L89
- [86] Tavecchio, F., Maraschi, L., & Ghisellini, G., 1998, *ApJ*, **509**, 608
- [87] Tavecchio, F., & Ghisellini, G., 2008, *MNRAS*, **385**, L98
- [88] Villata, M., & Raiteri, C. M., 1999, *A&A*, **347**, 30
- [89] Wagner, S., & Behera, B., 2010, 10th HEAD Meeting, Hawaii (*BAAS*, **42**, **2**, 07.05)
- [90] Weidinger, M., Rieger, M., & Spanier, F., 2010, *Astrophys. & Space Sciences Transactions*, **vol. 6**, Issue **1**, p. 1 (arXiv:1001.2145)
- [91] Zhang, Y. H., et al., 2002, *ApJ*, **572**, 762



3C66A
($z = 0.3$)

c)

